

GERDA Phase II: search for neutrinoless double beta decay

M. Agostini^a, A.M. Bakalyarov^m, M. Balata^a, I. Barabanov^k, L. Baudis^s, C. Bauer^g, E. Bellotti^{h,i}, S. Belogurov^{l,k}, A. Bettini^{p,q}, L. Bezrukov^k, J. Biernat^c, T. Bode^o, D. Borowicz^c, V. Brudanin^e, R. Brugnera^{p,q}, A. Caldwellⁿ, C. Cattadoriⁱ, A. Chernogorov^l, V. D'Andrea^a, E.V. Demidova^l, N. Di Marco^a, A. Domula^d, E. Doroshkevich^k, V. Egorov^e, R. Falkenstein^r, A. Gangapshev^{k,g}, A. Garfagnini^{p,q}, M. Giordano^a, C. Goochⁿ, P. Grabmayr^r, V. Gurentsov^k, K. Gusev^{e,m,o}, J. Hakenmüller^g, A. Hegai^r, M. Heisel^g, S. Hemmer^q, R. Hiller^s, W. Hofmann^g, M. Hult^f, L.V. Inzhechik^k, J. Janicskó Csáthy^o, J. Jochum^r, M. Junker^a, V. Kazalov^k, Y. Kermaidic^g, T. Kihm^g, I.V. Kirpichnikov^l, A. Kirsch^g, A. Kish^s, A. Klimenko^{g,e}, R. Kneißlⁿ, K.T. Knöpfle^g, O. Kochetov^e, V.N. Kornoukhov^{l,k}, V.V. Kuzminov^k, M. Laubenstein^a, A. Lazzaro^o, V.I. Lebedev^m, M. Lindner^g, I. Lippi^q, A. Lubashevskiy^{g,e}, B. Lubsandorzhev^k, G. Lutter^f, C. Macolino^a, B. Majorovitsⁿ, W. Maneschg^g, G. Marissens^f, M. Miloradovic^s, R. Mingazheva^s, M. Misiaszek^c, P. Moseev^k, I. Nemchenok^e, K. Panas^c, L. Pandola^b, K. Pelczar^a, A. Pullia^j, C. Ransom^s, S. Riboldi^j, N. Rumyantseva^{m,e}, C. Sada^{p,q}, F. Salamidaⁱ, C. Schmitt^r, B. Schneider^d, S. Schönert^o, J. Schreiner^g, O. Schulzⁿ, A-K. Schütz^r, B. Schwingenheuer^g, O. Selivanenko^k, E. Shevchik^e, M. Shirchenko^e, H. Simgen^g, A. Smolnikov^{g,e}, L. Stanco^q, L. Vanhoeferⁿ, A.A. Vasenko^l, A. Veresnikova^k, K. von Sturm^{p,q}, V. Wagner^g, A. Wegmann^g, T. Wester^d, C. Wiesinger^o, M. Wojcik^c, E. Yanovich^k, I. Zhitnikov^e, S.V. Zhukov^m, D. Zinatulina^e, A. Zschocke^r, A.J. Zsigmond^{*n}, K. Zuber^d, and G. Zuzel^c (The GERDA Collaboration)

^a) INFN Laboratori Nazionali del Gran Sasso and Gran Sasso Science Institute, ^b) INFN Laboratori Nazionali del Sud, ^c) Jagiellonian University, ^d) Technische Universität Dresden, ^e) Joint Institute for Nuclear Research, ^f) European Commission, JRC-Geel, ^g) Max-Planck-Institut für Kernphysik, ^h) Università Milano Bicocca, ⁱ) INFN Milano Bicocca, ^j) Università degli Studi di Milano e INFN Milano, ^k) Institute for Nuclear Research of the Russian Academy of Sciences, ^l) Institute for Theoretical and Experimental Physics, ^m) National Research Centre "Kurchatov Institute", ⁿ) Max-Planck-Institut für Physik, ^o) Technische Universität München, ^p) Università di Padova, ^q) INFN Padova, ^r) Eberhard Karls Universität Tübingen, ^s) Universität Zürich

E-mail: gerda-eb@mpi-hd.mpg.de

The GERDA (GERmanium Detector Array) experiment, located at the Laboratori Nazionali del Gran Sasso, is searching for neutrinoless double beta ($0\nu\beta\beta$) decay of ^{76}Ge . Since the end of 2015, in Phase II of the experiment, 35 kg of enriched high-purity germanium detectors are operated in liquid argon, that serves as cooling for the detectors as well as active shield against external radiation. The aim is a sensitivity on the $0\nu\beta\beta$ decay half-life larger than 10^{26} yr with about 100 kg·yr exposure and a background level of about 10^{-3} cts/(keV·kg·yr). An overview of the analysis of the data collected so far is presented with an emphasis on the background rejection techniques and their performance together with the half-life limit.

EPS-HEP 2017, European Physical Society conference on High Energy Physics
5-12 July 2017
Venice, Italy

*Speaker.

1. Introduction

Neutrino accompanied double beta ($2\nu\beta\beta$) decay has been observed for a number of isotopes for which a single beta decay is energetically is not allowed or strongly suppressed because of a large change of spin. In these isotopes it is possible to search for neutrinoless double beta ($0\nu\beta\beta$) decay that would appear as a peak at the Q -value of the $2\nu\beta\beta$ spectrum. The discovery of such a process would imply lepton number violation, the Majorana nature of the neutrino and give information about the absolute neutrino mass scale.

Already $2\nu\beta\beta$ decay is extremely rare with half-lives ranging from 10^{18} to 10^{24} years. The half-life of $0\nu\beta\beta$ decay is expected to be longer than about 10^{26} years which means that the radioactive background in the experiments searching for it must be extremely low. They need to maximize the active mass with isotope enrichment and eliminate radioactive backgrounds. In order to reduce the background from cosmic rays, the experiments are built in underground locations, with multiple layers of shielding against the natural environmental radiation. Additionally the materials used in the experimental setup have to be highly radio-pure and the detectors need to have a good energy resolution in order to reduce the intrinsic $2\nu\beta\beta$ decay background.

The GERDA experiment [1] searches for $0\nu\beta\beta$ decay of ^{76}Ge at a Q -value of $Q_{\beta\beta} = 2039$ keV using an array of isotopically enriched high purity germanium (HPGe) detectors. Germanium has the advantage that the detectors are at the same time the source for the $0\nu\beta\beta$ decay and their isotopic enrichment to up to 88% in ^{76}Ge is a well established process. Furthermore, HPGe detectors are intrinsically radio-pure and have an excellent energy resolution that make them fitting candidates for the $0\nu\beta\beta$ decay search. The operation of Ge detectors under ultra low background and cryogenic conditions and the protection of the material from cosmic activation during the production process present the challenges for the experiment.

The GERDA experiment is located at the Laboratori Nazionali del Gran Sasso of INFN that provides a rock overburden of about 3500 m water equivalent to reduce the cosmic background. The array is suspended in liquid argon (LAr) and the LAr cryostat is surrounded by a water tank to provide shielding against external radiation. Phase I of GERDA completed successfully in 2013 resulting in a ^{76}Ge $0\nu\beta\beta$ decay half-life limit of $T_{1/2} > 2.1 \cdot 10^{25}$ years (90% C.L.) [2]. In this paper, Phase II of the experiment is introduced with emphasis on background reduction techniques and the first results are presented [3].

2. Phase II of the GERDA experiment

The goal of GERDA Phase II is to increase the sensitivity by increased detector mass and by further reduction of the background coming from the close vicinity of the detectors. Broad energy germanium (BEGe) detectors were studied and produced for Phase II. This type of detectors have favorable pulse shape discrimination (PSD) properties, as described in the next section. In total GERDA is operating 40 detectors in an array of 7 strings in Phase II: 30 enriched BEGe detectors with a total mass of 20 kg produced for GERDA [4], 7 enriched semi-coaxial detectors with a total mass of 15.8 kg and 3 semi-coaxial detectors with natural isotopic composition with a total mass of 7.6 kg originating from previous experiments [5, 6]. In order to reduce the radioactivity in

the surrounding materials, the detector holders and contacts were upgraded to have a significantly lower mass with respect to Phase I.

One of the most important improvements in Phase II is coming from the fact that the LAr volume has been instrumented with light sensitive sensors. This enables an active vetoing (LAr veto) of events causing signals in both germanium and liquid argon. The LAr veto system consists of 16 photo-multipliers on the top and the bottom plates and a dense curtain of wavelength shifting fibers equipped with silicon photo-multipliers around the Ge detector array.

Data taking of Phase II started in Dec 2015 and it will be ongoing until the design exposure of about 100 kg·yr is reached. During data taking, all events that have an energy deposition in the $Q_{\beta\beta} \pm 25$ keV region in one of the Ge detectors are not processed until all the analysis cuts are finalized in order to ensure a blinded analysis. The first unblinding (Phase IIa) of the data corresponding to 10.8 kg·yr exposure took place in June 2016 [3] from which the analysis and results are described in the next sections. Until June 2017 an exposure of 34.5 kg·yr of data were collected and processed for analysis.

Data taking is running stably with continuous monitoring of the data taking conditions and the data quality. Every 1-2 weeks or in case of a change in the conditions, a calibration is taken using ^{228}Th sources lowered next to the Ge detector array. These calibrations are used to monitor and calibrate the energy scale of the Ge detectors and for the determination of pulse shape discrimination cuts. The shifts of the energy scale between consecutive calibrations are below 0.5 keV for most of the Ge detectors. This demonstrates the stability of the system. The achieved energy resolution at $Q_{\beta\beta} = 2039$ keV is (3.0 ± 0.2) keV and (4.0 ± 0.2) keV for BEGe and semi-coaxial detectors, respectively.

3. Background reduction techniques

The $0\nu\beta\beta$ decay signature is the energy deposition of the two electrons within one Ge detector without any signal in other Ge detectors, therefore events with energy depositions in multiple Ge detectors are rejected. This is called the anti-coincidence cut. In order to reject energy depositions caused by cosmic muons crossing the experiment a muon veto cut is applied: events in coincidence (within 8 μs) with a PMT signal in the water tank or in the plastic scintillators above the experiment are rejected. The measured energy spectrum after these cuts in the BEGe (left) and the semi-coaxial (right) detectors is shown in fig. 1 together with the fitted background model.

The background model is based on simulated signals from different background components around the detector array and then fitted to the data [7]. The screening results of the materials used in the construction are taken into account in the simulations. The main background components are ^{40}K , ^{42}K coming from ^{42}Ar in the LAr, intrinsic $2\nu\beta\beta$ decay of ^{76}Ge , ^{226}Ra from the ^{238}U series, ^{228}Ac , ^{232}Th series, ^{60}Co , and alphas from the ^{226}Ra decay chains. The background model fit can shed light on where the background sources come from and where they are distributed (cables, holders, mini-shroud, detector surface, or LAr volume). The spectral shapes vary with absorption length. From the fit the expected number of background events and their energy distribution in the region of interest around $Q_{\beta\beta}$ can be derived.

Events that have scintillation light detected in the LAr volume are rejected. This LAr veto cut suppresses the Compton continuum from a ^{228}Th source around 2039 keV by a factor of 100.

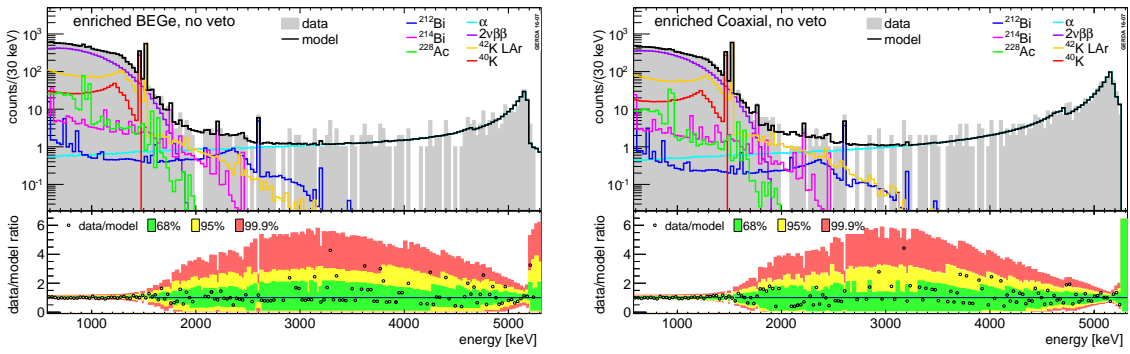


Figure 1: The measured energy spectrum of BEGe (left) and semi-coaxial (right) detectors corresponding to 5.8 kg·yr and 5.0 kg·yr of exposure, respectively. The spectra are shown after the detector anti-coincidence and muon veto cuts compared to the background model fit based on simulations.

The background suppression in physics data is shown in the left-hand side of fig. 2. The 1525 keV line from the ^{42}K beta decay is strongly suppressed since the electron produces scintillation light in the LAr. After comparing the Ge energy spectrum with the simulated signal from $2\nu\beta\beta$ decay using the measured half-life, it is verified that after the LAr veto cut about 97% of the events in the 600-1300 keV region come from $2\nu\beta\beta$ signal. Using random coincidences with test pulser events the $0\nu\beta\beta$ signal acceptance of the LAr veto cut was determined to be $(97.7 \pm 0.1)\%$.

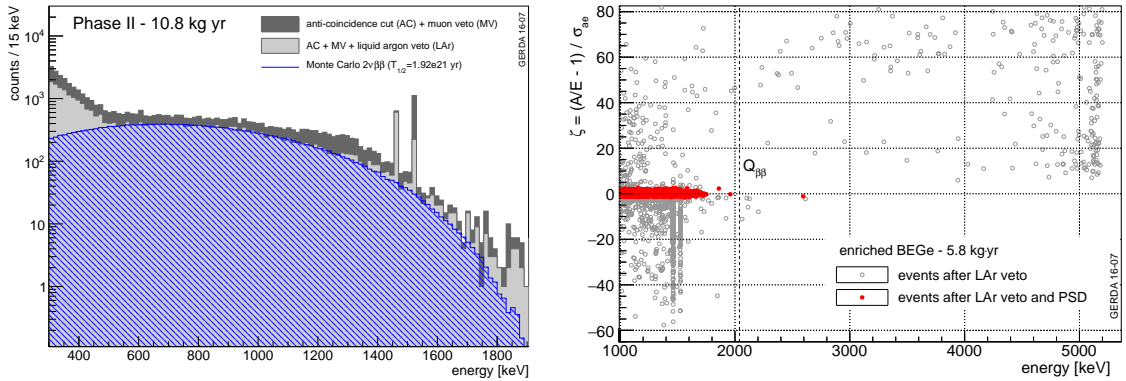


Figure 2: *Left:* The spectrum before and after applying the LAr veto cut compared to simulated $2\nu\beta\beta$ decay spectrum. *Right:* PSD classifier of BEGe detectors as a function of energy for events that passed the LAr veto cut.

Finally, background events producing multiple energy depositions within one Ge detector, called multi-site events (MSEs), are separated using pulse shape analysis from single-site events (SSEs), like the $0\nu\beta\beta$ decay where both electrons deposit their energy within approximately 1 mm^3 of the detector volume. Due to their detector geometries the BEGe and the semi-coaxial detectors have different pulse shapes and are treated separately based on the same methods as used in Phase I [8].

In BEGe detectors the electric field and the weighting potential have a special shape thanks to the small p+ contact size. This results in similar pulse shapes of SSEs independent of the location of the energy deposition within a large fraction of the detector volume. This allows a one-parameter PSD cut based on the amplitude of the current pulse divided by the energy, called A/E . The A/E

parameter is lower for MSEs than for SSEs and higher for alpha events close to the p+ contact, thus a two-sided cut is applied to the data from the BEGe detectors to reject background events. The calibration data with ^{228}Th source is used to determine the cut values and corrections for instabilities in time and for energy dependence of A/E . In the right-hand side of fig. 2 the PSD classifier based on the A/E parameter after corrections is shown as a function of energy. All high energy alpha events are rejected by the high cut and the peaks of ^{40}K and ^{42}K are suppressed by the low cut due to the relatively large fraction of multiple Compton scattering events. The $0\nu\beta\beta$ signal acceptance is estimated to be $(87 \pm 2)\%$ based on calibration data and $2\nu\beta\beta$ events.

In the semi-coaxial detectors the charge pulse has no simple shape, thus a more sophisticated pulse shape analysis is necessary. The time distribution of the signal is used as input variables to two artificial neural networks (ANNs) in order to separate SSE from MSE and surface alpha events. The training for MSE classification is performed on calibration data and cross checked with simulations. For the surface alpha rejection the $2\nu\beta\beta$ events after LAr veto cut are used as signal and events above 3500 keV are used as background sample in the training of the second ANN. The combined $0\nu\beta\beta$ signal acceptance is estimated to be $(79 \pm 5)\%$.

4. Results and outlook

The final energy spectra after the LAr veto and PSD cuts are shown in fig. 3. The background index is calculated in the analysis window in the 1930-2190 keV region excluding the intervals 2104 ± 5 keV and 2119 ± 5 keV, which correspond to known peaks predicted by the background model. In the semi-coaxial detectors 4 events remain after all cuts that corresponds to a background index of $3.5^{+2.1}_{-1.5} \cdot 10^{-3}$ counts $\text{keV}^{-1}\text{kg}^{-1}\text{yr}^{-1}$, while in the BEGe detectors only one event remains corresponding to $0.7^{+1.1}_{-0.5} \cdot 10^{-3}$ counts $\text{keV}^{-1}\text{kg}^{-1}\text{yr}^{-1}$. This shows that the background goal of Phase II is reached with the BEGe detectors, which corresponds to less than one expected background event at $Q_{\beta\beta}$ within one FWHM until the design exposure of 100 kg·yr.

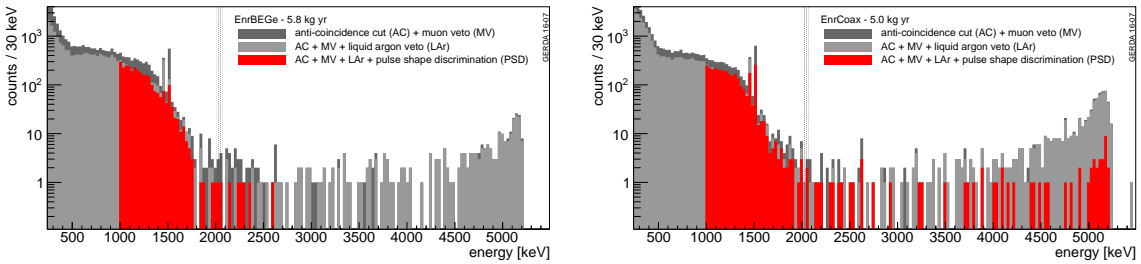


Figure 3: The measured energy spectrum of BEGe (left) and semi-coaxial (right) detectors after the different background rejection cuts.

A combined unbinned profile likelihood fit of the spectrum from the Phase I and Phase IIa data sets was performed in the analysis window assuming a flat background and a gaussian signal at $Q_{\beta\beta}$. The spectra in the region of interest are shown in fig. 4. The best fit resulted in a half-life limit for the $0\nu\beta\beta$ signal of $T_{1/2} > 5.3 \cdot 10^{25}$ yr (90% C.L.). The median sensitivity assuming no signal is $4.0 \cdot 10^{25}$ yr. For light Majorana neutrino exchange the half-life limit converts to a limit on the effective Majorana neutrino mass of $m_{\beta\beta} < 0.15 - 0.33$ eV (90% C.L.) depending on the nuclear matrix element for ^{76}Ge used in the calculation.

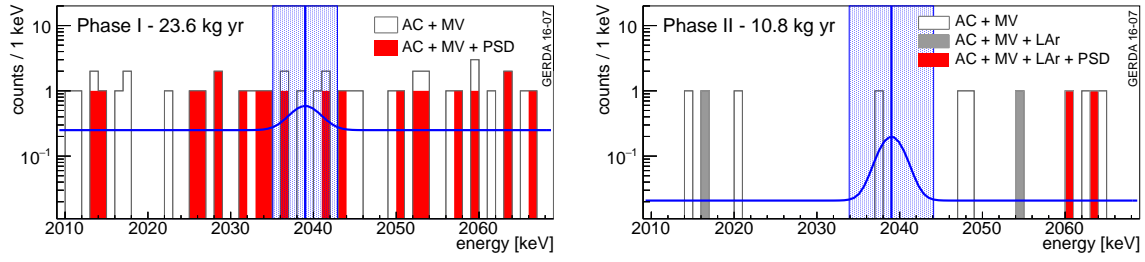


Figure 4: The energy spectrum in the region of interest from Phase I (left) and Phase II (right) data after all background rejection cuts (red histograms) together with the fit including a hypothetical signal corresponding to the 90% C.L. limit of $T_{1/2} > 5.3 \cdot 10^{25}$ yr.

In summary, GERDA Phase II is currently taking data with 35.8 kg of enriched germanium detectors in order to reach the design exposure of 100 kg·yr. The design goal for the background level of 10^{-3} counts $\text{keV}^{-1}\text{kg}^{-1}\text{yr}^{-1}$ was accomplished with the BEGe detectors thus GERDA will reach a sensitivity of the order of 10^{26} yr for the half-life within 3 years of operation. For the future of the $0\nu\beta\beta$ decay search with ^{76}Ge a ton scale experiment called LEGEND [9] is planned. LEGEND is a joint effort from the GERDA and MAJORANA collaborations including new members and is organized in two stages: first a 200 kg experiment in the current GERDA cryostat at LNGS and then a 1000 kg experiment in a new location with an improved background index.

References

- [1] GERDA Collaboration (K.-H. Ackermann *et al.*), *Eur. Phys. J. C* **73** (2013) 2330 [arXiv:1212.4067]
- [2] GERDA Collaboration (M. Agostini *et al.*), *Phys. Rev. Lett.* **111** (2013) 12 [arXiv:1307.4720]
- [3] GERDA Collaboration (M. Agostini *et al.*), *Nature* **544** (2017) 47 [arXiv:1703.00570]
- [4] GERDA Collaboration (M. Agostini *et al.*), *Eur. Phys. J. C* **75** (2015) 39 [arXiv:1410.0853]
- [5] Heidelberg-Moscow Collaboration (H.V. Klapdor-Kleingrothaus *et al.*), *Eur. Phys. J. A* **12** (2001) 147
- [6] IGEX Collaboration (C.E. Aalseth *et al.*), *Phys. Rev. D* **65** (2002) 092007
- [7] GERDA Collaboration (M. Agostini *et al.*), *Eur. Phys. J. C* **74** (2014) 2764 [arXiv:1306.5084]
- [8] GERDA Collaboration (M. Agostini *et al.*), *Eur. Phys. J. C* **73** (2013) 2583 [arXiv:1307.2610]
- [9] LEGEND Collaboration (N. Abgrall *et al.*), *Proceedings of the MEDEX'17 meeting* [arXiv:1709.01980]